

# Experimental Profiles of the Balmer Line $H\beta$ Emitted from an Afterglow Plasma Without and With a Superposed Magnetic Field up to 10 Tesla

H. W. Drawin and J. Ramette

Association Euratom-CEA sur la Fusion, Département de Physique du Plasma et de la Fusion Contrôlée, Centre d'Etudes Nucléaires, Fontenay-Aux-Roses (France)

Z. Naturforsch. **34 a**, 1041–1050 (1979); received May 14, 1979 \*

The profile of the  $H\beta$  line emitted from an afterglow plasma in pure hydrogen gas and a mixture of hydrogen and helium has been measured in axial direction using a multichannel spectrum analyzer with additional temporal resolution. Measurements were performed without and with a superposed magnetic field ( $B \leq 10.8$  Tesla) in axial direction. With magnetic field we observed a rather strong dependence of the wavelength positions of the two lateral "Zeeman components" (intensity maximum due to combined Stark-Zeeman effects). This feature is important in radiative transfer calculations and for the spectroscopic determination of magnetic fields in plasmas. — Both with and without magnetic field we always observed a line structure superposed on the  $H\beta$  profile. The structure disappeared in an active electrical discharge and changed with gas composition. The line structure is interpreted as being due to electronic transitions of molecular hydrogen. It is very probable that the "satellite structures" of Balmer lines observed by other authors under quite different experimental conditions and interpreted as dynamical Stark effect splitting due to fluctuating electric fields have in most cases the same molecular origin. Our earlier published line profiles of  $H\beta$  for  $B = 0$  [J. Ramette and H. W. Drawin, Z. Naturforsch. **31 a**, 401 (1976)] are revised in the present paper.

## 1. Introduction

Spectral lines emitted by a plasma of sufficiently high electron density  $N_e$  and confined by a strong magnetic field of induction  $B$  are broadened by combined Stark and Zeeman effects. The knowledge of the line profiles as a function of  $N_e$ ,  $B$ , and heavy particle and electron temperatures,  $T_H$  and  $T_e$ , is important for fundamental line broadening studies and for practical applications, for instance for determining  $N_e$  in laboratory and astrophysical plasmas containing magnetic fields, radiative transfer calculations for magnetized plasmas, determination of strength and polarization of magnetic fields. Concerning this latter point it is to be noted that Stark effect modifies the position of the Zeeman components, as will be discussed later.

The knowledge of Stark-Zeeman broadened line profiles is still rather scarce and studies on this subject matter are still in the first beginning. The first theoretical studies were by Maschke and Voslamber [1] who calculated the profile of the hydro-

gen Ly  $\alpha$  line for the special case that the three Zeeman components in the case of Paschen-Back effect are separated by a sufficiently strong magnetic field and that their Stark profiles do not overlap (the conditions chosen were  $N_e = 1 \cdot 10^{14} \text{ cm}^{-3}$ ,  $B = 4.5$  Tesla to 5.5 Tesla). More comprehensive calculations have been performed by Nguyen-Hoe et al. [2–6] for the lines Ly  $\alpha$ , Ly  $\beta$  and  $H_\alpha$  for electron densities ranging from  $10^{15} \text{ cm}^{-3}$  to  $10^{18} \text{ cm}^{-3}$  and for  $B$ -values up to 12 Tesla. Their papers contain numerous tables and graphical representations of those line profiles. The combined Stark-Zeeman broadening was also considered by Aleksin and Fesenko [6] who studied the possible changes of line profiles in a strong magnetic field without giving any detailed numerical or graphical results.

A special situation arises when the atom velocity  $v$  and the magnetic induction  $B$  are so high that the Lorentz electric field strength  $E_L = v \times B$  becomes larger than the normal Holtsmark field strength

$$F_0 = 2.6 e_0 N_e^{2/3} = F_0(N_e) \quad (1)$$

of the quasi-static microfield. In this case — to our knowledge the first time pointed out in Refs. [7–8] — the profile is mainly determined by the Zeeman splitting and the velocity distribution of the atoms which causes Doppler effect and the velocity dependent Stark effect due to the Lorentz field. Figure 1 shows  $F_0 = F_0(N_e)$  and the mean Lorentz

\* Reception of the first version January 29, 1979.

Reprint requests to Mons. H. W. Drawin, Association Euratom-CEA, Département Fusion, Centre d'Etudes Nucléaires, Boite Postale N. 6, F-92260 Fontenay-Aux-Roses, Frankreich. 0340-4811 / 79 / 0900-1041 \$ 01.00/0

Please order a reprint rather than making your own copy.



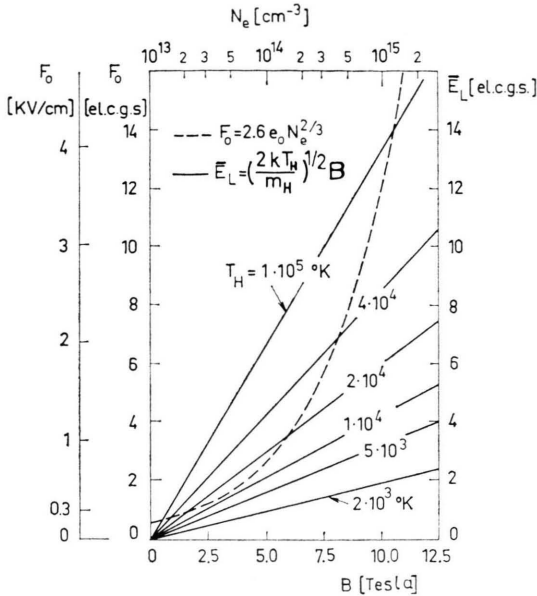


Fig. 1. Normal electric microfield strength  $F_0$  as a function of electron density  $N_e$ , and mean Lorentz electric field strength  $\bar{E}_L$  as a function of magnetic induction  $B$  with the temperature  $T_H$  as a parameter (after Ref. [7]).

field strength  $\bar{E}_L$  experienced by hydrogen atoms moving perpendicular to  $B$  with a velocity  $v_{\max}$  which corresponds to the maximum of the Maxwell distribution\* at temperature  $T_H$ :

$$\bar{E}_L = v_{\max} B = (2 k T_H / m_H)^{1/2} B. \quad (2)$$

For low  $N_e$  and high  $B$  and  $T_H$  values,  $\bar{E}_L$  always exceeds  $F_0$ . This special case (which applies for instance to Tokamak plasmas and many high-temperature low-density astrophysical objects) was considered by Galushkin [9] and Isler [10] who studied theoretically the modification of the  $H_\alpha$  [9, 10] and  $H_\beta$  [9] profiles due to the Lorentz field.

For a given  $B$ , the study of line profiles simultaneously broadened by microfield electric Stark and externally imposed Zeeman effects thus requires either relatively high  $N_e$  values or low temperatures, or both. Such measurements on  $H_\alpha$ ,  $H_\beta$ ,  $H_\gamma$  and  $H_\delta$  were performed by Drawin *et al.* [8, 11] and Nguyen-Hoe *et al.* [2, 5], and on the HeI,  $\lambda = 5876 \text{ \AA}$  line by Belland *et al.* [12]. Due to the relatively large  $N_e$  values in those experiments, the

microfield electric Stark effect was always the dominant broadening mechanism for  $H_\beta$ ,  $H_\gamma$  and  $H_\delta$ .

In order to extend the experimental domain to a region where the Zeeman effect dominates the gross structure of the  $H_\beta$  profile we set up an afterglow experiment coupled with a multi-channel spectrum analyzer. This kind of experiment would permit to observe in a single shot the profile for a large range of  $N_e$  and especially to study the transition from a mainly Stark-effect broadened profile to a mainly Zeeman-split line. As corresponding line profile calculations for Balmer lines other than  $H_\alpha$  do not yet exist, such measurements would also be of interest for future theoretical work.

The measurements showed a relatively strong dependence of the wavelength position of the Zeeman components from the electron density. This has consequences for the determination of magnetic fields from Zeeman splitting. However, no quantitative statements could be made about the form of the near and far line wings due to the presence of an unexpected irregular line structure superposed on the Zeeman-Stark broadened line and in this form not yet reported by other authors.

The present paper contains the essential results of our measurements and its possible consequences with regard to the measurement of plasma turbulence.

## 2. Experimental

The plasma was created in a linear discharge tube surrounded by a magnetic coil. The electrical energy for both the plasma and the magnetic field was delivered by condenser bancs. Since the energy stored is limited, we used coils with different internal diameter and length and consequently discharge tubes of smaller dimensions for the high magnetic fields than for the low ones. The form of the discharge tubes used is schematically shown in Fig. 2 with the dimensions given in Table 1.

In order to avoid axial inhomogeneity of the magnetic field strength the latter was continuously measured during the manufacturing process of the coils.

	Tube No. 1	Tube No. 2	Tube No. 3
$\phi$	25	25	10
$L_1$	500	200	100
$L_2$	515	225	120

Table 1. Dimensions of discharge tubes, in mm.

\* For particles moving with (one-dimensional) mean thermal velocity perpendicular to  $B$ ,  $v_{\max}$  has to be replaced by  $\langle v \rangle = (k T_H / 2 \pi m_H)^{1/2}$  of a gaussian distribution. The choice is in any case arbitrary, since the whole distribution function intervenes.

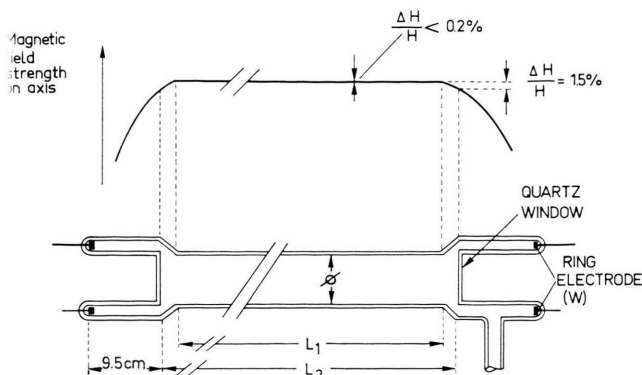


Fig. 2. Form and dimensions of discharge tubes used in the experiments. Also is shown the axial form of the magnetic field.

At both ends additional windings were added to ensure perfect axial field homogeneity in the plasma region proper. Figure 2 shows the form of the field along the axis of the discharge tube.

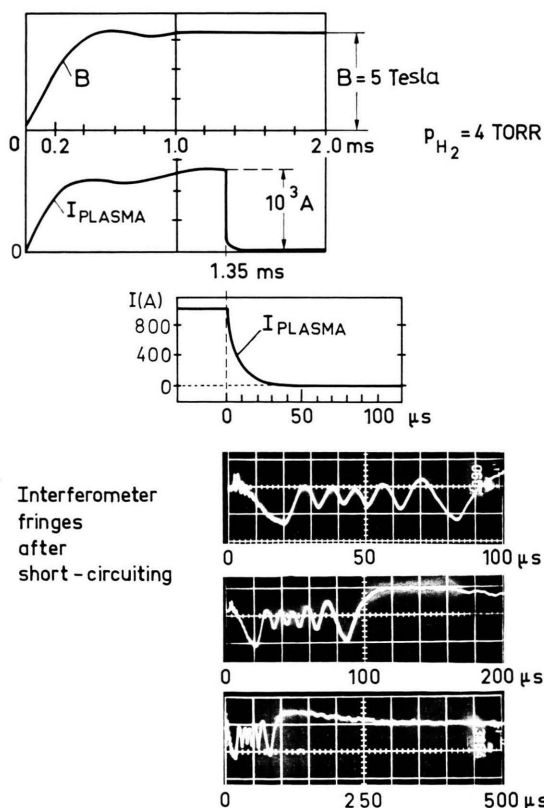


Fig. 3. Temporal evolution of plasma current and magnetic induction (upper part). Also are shown on a magnified time basis: the plasma current after short-circuiting and the same interferometer fringes displayed with three different time bases (lower part).

For the discharges we used pure hydrogen gas (purification by diffusion through a heated palladium membran).

In order to obtain a constant magnetic field during the whole afterglow phase we applied a L-C-delay line. The general lay-out of the electrical circuits was quite similar to the one shown in Fig. 2 of [8]. Figure 3 shows as an example the temporal evolution of plasma current and magnetic induction for a typical experiment. Short-circuiting of the plasma current is at  $t = 1.35$  ms which is considered as the beginning ( $t_0 = 0$ ) of the afterglow phase.  $40 \mu\text{s}$  after short-circuiting the plasma current was definitely zero.

All optical measurements were made along the axis of the discharge tube. A detailed description of the optical arrangement is given in [13].

For  $t > t_0$ ,  $N_e$  was measured by means of a He-Ne laser interferometer working at wavelength  $\lambda = 3.39 \mu$ . Figure 3 shows as an example measured fringes for a plasma recombining in a field of 5 Tesla. For the different experiments the plasma currents before short-circuiting varied between 1 kA and 2.5 kA.

The line profiles were measured by means of a 10-channel analyzer system, the band width covered by one channel being  $0.10 \text{ \AA}$ . The performance of this system is described in Refs. [13, 14]. Since all ten channels together cover only  $1 \text{ \AA}$  for a given position of the measuring head, the latter had to be displaced in order to obtain the whole profile from a series of shots under identical discharge conditions. This apparent disadvantage is largely compensated by the possibility to measure continuously the intensity of every channel during the whole afterglow.

### 3. Experimental Results

#### 3.1. Measurements with Magnetic Field

The line profiles obtained from a larger number of measurements are given in Figs. 4 to 7. For  $B = 3.5$  Tesla (Fig. 4) and  $B = 5.0$  Tesla (Fig. 5) we present only the line center and the blue wing. The red wings are of similar hatched structure but without showing any symmetry with respect to the line center. The profiles measured for  $B = 10.8$  Tesla are shown in Figures 6 a, b.

The most striking feature is the presence of many unexpected "peaks" distributed in an irregular man-

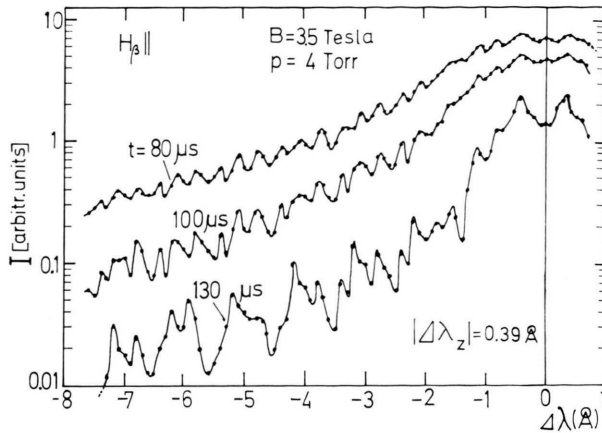


Fig. 4. Blue wing and center of  $H_\beta$  at different times after short-circuiting. Filling pressure was  $p = 4$  Torr  $H_2$ . Magnetic induction  $B = 3.5$  Tesla. Tube No. 2.

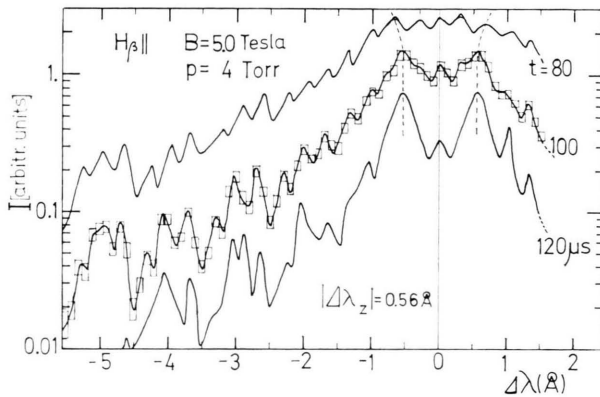


Fig. 5. Blue wing and center of  $H_\beta$  for  $B = 5$  Tesla. Filling pressure was 4 Torr  $H_2$ . Tube No. 2.

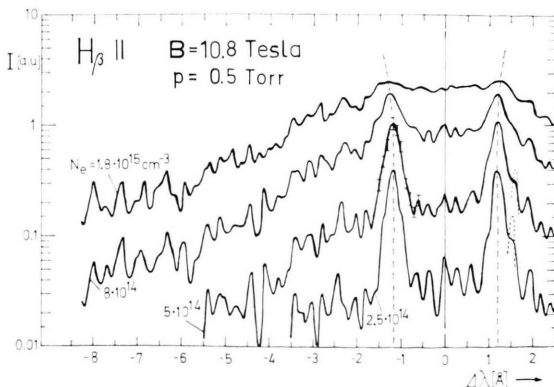


Fig. 6a

Fig. 6.  $H_\beta$  profile for  $B = 10.8$  Tesla; a) blue wing and line center; b) red wing. Filling pressure  $p = 0.5$  Torr  $H_2$ . Tube No. 3.

ner over the whole profile. These peaks appear briefly after short-circuiting of the plasma current. They occur first in the very far line wings. With increasing time  $t$ , the peak structure approaches more and more the central part of the line. During the first  $100 \mu s$  the peak structure changes smoothly with time without showing any characteristic dependence on electron density. For later times and for a given value of  $B$  the wavelengths of the peaks remain practically constant, only weak intensity variations occur. We made measurements for very different filling pressures and plasma currents. No significant modification of the gross satellite structure was found and no significant dependence of peak positions from electron density could be detected, apart from the one for the Zeeman components (see later). For identical discharge and magnetic field conditions the measurements are completely reproducible. In Figs. 5 and 6a we have indicated on a middle curve the region over which the measured intensities scatter. The mean errors are smaller. There is no doubt that the observed structure is a real feature.

The second feature that strikes is the electron density-dependent structure in the line center. In order to show this in more detail we give in Fig. 7 the central line structure for closely spaced time intervals from  $t = 50 \mu s$  to  $t = 130 \mu s$  after short-circuiting, at a magnetic induction of  $B = 5$  Tesla. The seven curves referring to  $60 \mu s, 70 \mu s, \dots, 130 \mu s$  have been composed from the oscilloscope traces of only three successive shots. For each shot the measuring head of the analyzer system was set on a pre-chosen position. The rectangles indicate where

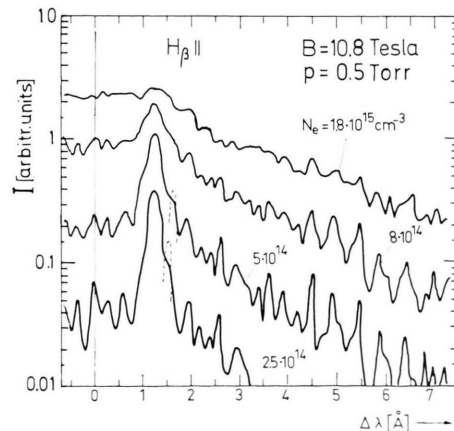


Fig. 6b



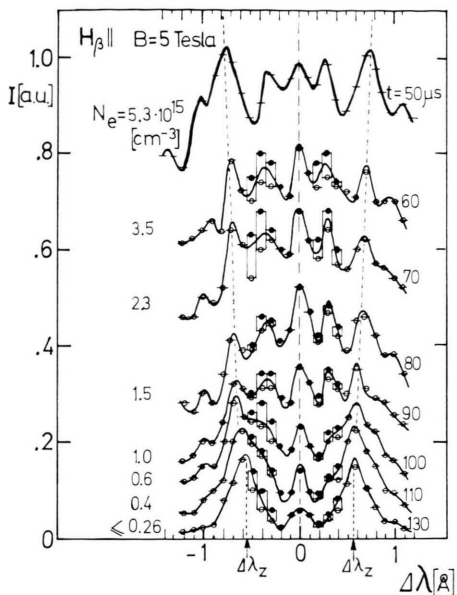


Fig. 7. Central part of  $H_\beta$  at different times  $t$  after short-circuiting. Magnetic induction  $B = 5$  Tesla. Filling pressure  $p = 2$  Torr  $H_2$ . Tube No. 2.

the intensities of two successive shots overlap. Open and full circles pertain to different shots. The curve for  $50 \mu s$  has been composed from independent measuring series. This figure also shows the good reproducibility of the measurements.

The  $\sigma^-$  and  $\sigma^+$  Zeeman components shall appear at wavelength distances  $\Delta\lambda_z = \pm 0.56 \text{ \AA}$  when  $B = 5$  Tesla. This is indeed the case for the profile at  $t = 130 \mu s$ . For all earlier times, i. e. at higher electron densities, the “Zeeman splitting” is larger and  $N_e$ -dependent. For  $N_e = 5.3 \cdot 10^{15} \text{ cm}^{-3}$  and  $B = 5$  Tesla we obtain a peak separation of  $\pm 0.75 \text{ \AA}$ . For comparison: the intensity shoulders of a purely Stark-broadened  $H_\beta$  line have at  $N_e = 5.3 \cdot 10^{15} \text{ cm}^{-3}$  a distance of  $\Delta\lambda_s = \pm 1.2 \text{ \AA}$  from the line center [26]. Quite a similar increase of the “Zeeman displacement” with  $N_e$  is observed for the other values of  $B$ , see Figures 5 and 6.

Apart from the “Zeeman components” we observed a peak structure whose intensity changes in the course of time. The wavelength positions of the individual peaks stay constant within the experimental uncertainty. A purely Zeeman splitted line observed parallel to the magnetic field direction — as it is in our case — should give rise to a Zeeman doublet only. In contrast to this we observe at all times a secondary maximum at the undisplaced

position  $\Delta\lambda = 0$ ; during some time ( $60 \mu s$  to  $90 \mu s$ ) its intensity exceeds the one of the lateral Zeeman components.

Figure 7 shows between the two “Zeeman components” two other weaker intensity maxima at  $\Delta\lambda = 0.29$  and  $\Delta\lambda = 0.32 \text{ \AA}$ . This finding is confirmed by the measurements for  $B = 10.8$  Tesla (Figs. 6 a, b) which show now two additional peaks (i. e. five intensity maxima) between the two “Zeeman components”, which for  $B = 5$  Tesla nearly coincided with the Zeeman peaks in Fig. 7, see also Figure 5. Also the measurements displaced in Fig. 4 agree with this finding: there is only one true maximum at  $\Delta\lambda = 0$  between the two Zeeman components, but the two intensity shoulders of the inner wings of the Zeeman components (curve  $t = 130 \mu s$  of Fig. 4) probably represent the two peaks resolved at  $B = 5$  Tesla (Figure 7).

In Figs. 6 a, b, the Zeeman components show intensity shoulders. We only succeeded to resolve a peak in the red wing of the red Zeeman component (see broken intensity maximum in Figs. 6 a, b) in displacing the measuring head in fractions of a channel width in the focal plan between successive shots. Positioning was critical.

No clear  $N_e$ - and  $B$ -dependence of the positions of the many individual peaks could be extracted from our measurements. In order to get additional information, measurements were made without a confining magnetic field.

### 3.2. Measurements Without Magnetic Field

The essential results for a pure hydrogen plasma have been summarized in the Figures 8 and 9. Figure 8 shows profiles at different times  $t$  after short-circuiting. As in the case with magnetic field, the peak structure increases in intensity in the course of the afterglow phase. The position of the individual peaks is practically independent of time, i. e. independent of  $N_e$ , but the intensities are a function of the gas pressure. This is demonstrated in Figure 9. The letters A, B, C refer to three different shots made at three different filling pressures  $p$  (A:  $p = 2.5$  Torr; B:  $p = 5$  Torr; C:  $p = 7.5$  Torr) without changing the position of the measuring head. The peak structure clearly increases with  $p$ . This is a strong indication that the peak structure might originate from molecules. Quite a similar phenomenon was observed when we measured the profile of the He line at  $\lambda = 4471.5 \text{ \AA}$ , see Ref. [14].

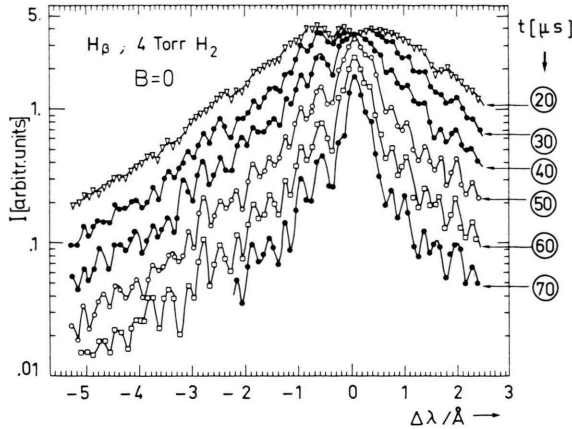


Fig. 8.  $H_\beta$  profile emitted from a pure hydrogen plasma without magnetic field. Identical results for Tubes No. 1 and 2.

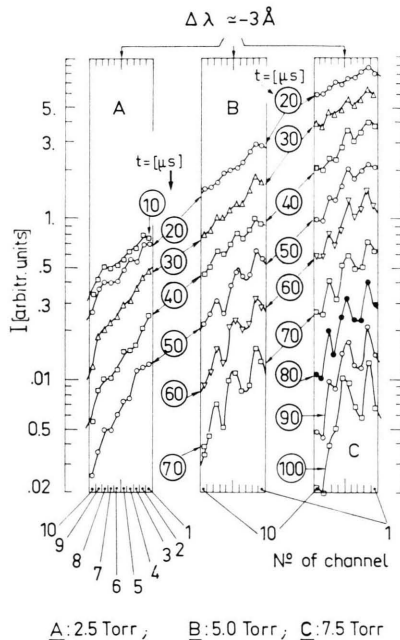


Fig. 9. Intensity distribution measured in the blue wing at different filling pressures; A:  $p = 2.5$  Torr, B:  $p = 5.0$  Torr, C:  $p = 7.5$  Torr  $H_2$ . Tube No. 1. No magnetic field.

In order to clarify this point, two different experiments were performed. In the first one we added a trace of hydrogen to helium gas and measured  $H_\beta$  during the afterglow. Figure 10 shows a corresponding profile. The line contour is different from the one for a pure hydrogen plasma. A peak structure is observed but the wavelengths of the relatively weak peaks occur at other wavelengths. There is much similarity with the  $H_\beta$  profile measured by Burgess and Mahon [15] for 0.01%  $H_2$  in helium.

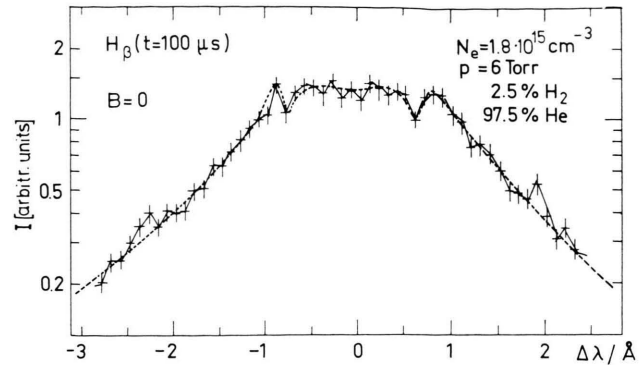


Fig. 10. Emission profile of  $H_\beta$  from a helium afterglow plasma containing 2.5%  $H_2$ . Tube No. 1. No magnetic field.

We believe that the peak structure and especially the form of the line center have in both cases the same origin.

For the second experiment we modified the electrical circuit in order to obtain an aperiodic oscillation of the plasma current (see insertion in Figure 11).  $H_\beta$  profiles measured at  $t = 1.0$  ms and  $t = 1.4$  ms are shown in Figure 11. At 1 ms the current is still 200 Amp. Although pure hydrogen was used no peak structure appeared. The profile for  $t = 1.4$  ms (plasma current still 60 Amp.) begins to show slight irregularities which might be the first sign of the development of the peak structure. The non existence of a well discernable peak structure for the current driven afterglow is probably due to the fact that the gas temperature is held on a sufficiently high level to avoid the formation of elec-

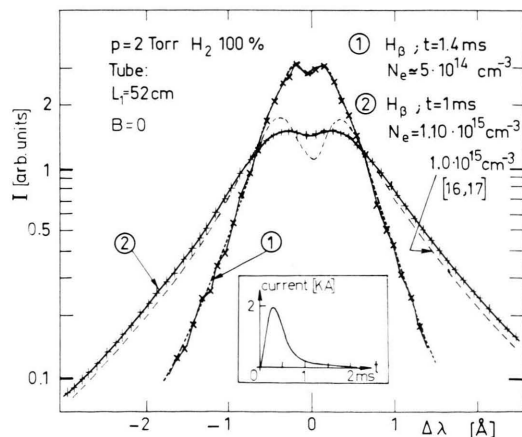


Fig. 11.  $H_\beta$  profiles emitted from a current-driven afterglow plasma (pure hydrogen gas). For comparison, a theoretical Stark profile after Refs. [17–18] for  $N_e = 1.10^{15} \text{ cm}^{-3}$ . Insertion shows the plasma current as a function of time.

tronically excited molecules. On the other hand, such molecules are easily formed in a currentless afterglow plasma in which the temperature drops rapidly far below 5000 °K (see for instance Fig. 3 in Ref. [18]).

## 4. Interpretation

### 4.1. The Superposed Line Structure

The line structure superposed on the profile of the  $H_\beta$  line both with and without magnetic field is very probably due to  $H_2$  molecular transitions. This interpretation is strongly supported by a comparison of the measured wavelengths of the “peaks” with those listed by Crosswhite [19]. This comparison is undertaken in Fig. 12 for our measurements without magnetic field. The  $H_\beta$  profile with the superposed line structure presented in Fig. 12 refers to the same initial experimental conditions as the curves in Fig. 8 with the only difference that the intensities have been evaluated at  $t = 100 \mu\text{s}$  after short-circuiting of the plasma current. At this late time the individual peaks are much better resolved than during the earlier times. Above each peak we have indicated the wavelengths of the  $H_2$  molecular lines as given by Crosswhite. Within the experimental uncertainty of our measuring device there is agreement with Crosswhite’s wavelengths values, with the exception of one irregularity — probably a not resolved peak — at  $\lambda \cong 4861.05 \dots 4861.15 \text{ \AA}$  (see arrow). A still stronger shoulder on the red wing of  $H_\beta$  corresponds to the strong, not resolved

$H_2$  molecular lines between 4861.637 and 4861.847 Å.

The relative peak intensities do not in all cases correspond to those published by Crosswhite. This might be due to the quite different thermodynamic conditions under which Crosswhite’s measurements were made. His observations refer to (1) a low-temperature (77 K) low-pressure (0.1 – 0.2 Torr) electrodeless discharge of low and medium power; (2) a high-power microwave discharge at 1 Torr; and (3) a high-power electrodeless discharge with a pressure of 80 Torr in order to suppress high vibrational quantum numbers. The intensities are “eye estimates” and have no quantitative character. For a comprehensive literature survey on the  $H_2$  level system see e. g. Sharp [20].

The temporal resolution of the spectra clearly shows that the thermodynamic state intervenes in the relative peak intensities. This is shown in Figure 12. On the right side we have presented for the ten measuring channels the intensities emitted from the same afterglow at times  $t = 50, 70$ , and  $100 \mu\text{s}$  after short-circuiting. At  $50 \mu\text{s}$ , the largest intensity is measured on channel No. 5 and the relative intensities of the peaks agree roughly with the not entirely resolved group of  $H_2$  molecular lines at  $\lambda = (4864.460), 4864.911, 4865.134, 4865.295$ , and  $4865.460 \text{ \AA}$  as published by Crosswhite. However, at  $t = 100 \mu\text{s}$  the largest intensity is found on channel No. 6 at  $4865.15 \text{ \AA}$ . Since there is no impurity line at this wavelength, we interpret this peak as the  $H_2$  molecular line at  $4865.134 \text{ \AA}$ .

If the thermodynamic state intervenes in the relative peak intensities, successively following rotational lines of the same branch should approximately have the same intensity. In the spectral region of interest, the lines  $4861.734 \text{ \AA}$  and  $4862.760 \text{ \AA}$  represent the  $N=2$  and  $N=4$  lines of the same  $Q$ -branch. The measured peak intensities do not contradict this fact.

We conclude that the measured peak structure has its origin in  $H_2$  molecular transitions.

On the basis of these findings it is very likely that also the peak structure found in the presence of a magnetic field has its origin in transitions of the hydrogen molecule but additionally submitted to Zeeman (and Stark) effect. There is only few work done on the Zeeman effect of molecules. The last review dates back to 1934 (Crawford [21]). The summary given by Herzberg [22] is based on Refs.

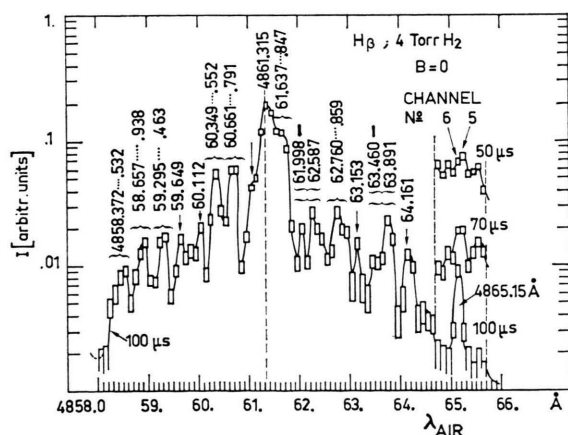


Fig. 12. Comparison of measured peak structure with wavelength positions of  $H_2$  after [19]. The initial experimental conditions are the same as for Figure 8.

[21], [23–24]. Practically all work is limited to electronic doublet states [25], the simplest case of all but which does not apply to  $H_2$ .

For the magnetic field strengths encountered in our experiment, molecules should show Paschen-Back effect and uncoupling of the spin vector  $S$  from the internuclear axis (pp. 151–152 of Ref. [24], pp. 303–304 of Ref. [22]) leading in principal to a new line pattern and intensity distribution of the molecular spectrum compared to the magnetic field-free case. Indeed, the energy splitting of a molecular level is given by (Eqs. (V.86) and (V.93) of Ref. [22]):

$$\Delta E = \left[ \frac{A^2 M_K}{K(K+1)} + 2 M_S \right] \frac{e_0 h}{4 \pi m_e c} B \quad (3)$$

where  $A$  and  $K$  are the quantum numbers in Hund's case (b), and  $M_K$  and  $M_S$  are the projections of  $\mathbf{K}$  and  $\mathbf{S}$  in the direction of  $B$ . Thus, owing to the selection rules  $\Delta M_S = 0$ ,  $\Delta M_K = \pm 1.0$  for Paschen-Back effect, the splitting of a molecular line rapidly decreases with increasing  $K$  (i.e. with increasing rotational quantum number  $N$ ), and for singlet states ( $A = 0$ ) there is no splitting at all. This would explain the relative insensitivity of the positions of the peaks between the Zeeman components with regard to magnetic field strength. Only those lines pertaining to small values of  $K$  would show (small) Zeeman splitting. The different structure in the line wings with and without magnetic field might be due to this effect.

Since the level assignment of the many  $H_2$  molecular lines is still open it is not possible to calculate their Zeeman splitting. Once all  $H_2$  molecular transitions are known it should in principle be possible to predict their Zeeman spectrum and to explain the difference between the structures found with and without magnetic field, provided the satellite structure originates from hydrogen molecules.

#### 4.2. Position of "Zeeman Components"

The  $N_e$ -dependent position of the "Zeeman doublet" of the atomic line arises from the competitive actions of the electric and magnetic fields interacting with the atom. In the case of vanishing electric field and pure Paschen-Back-effect one obtains the three pure Zeeman components at wavelength distances

$$\Delta \lambda_z = \pm \lambda_0^2 \frac{e_0}{4 \pi m_e c} B, \text{ and } 0 \quad (4)$$

from the unperturbed wavelength at  $\lambda_0$ . Especially for  $H_\beta$  one has for the two outer components (Zeeman doublet):

$$\Delta \lambda_z = \pm 0.112 \cdot B \text{ \AA} \quad (5)$$

with  $B$  in Tesla (1 Tesla  $\cong 10^4$  gauss). Superposition of an electric field leads to additional splitting. For a given  $B$ , a superposed constant electric field  $F$  will split up the pure Zeeman components in a combined Stark-Zeeman pattern which is different for observation parallel and perpendicular to the direction of  $B$ . After integration over the probability function  $W(F/F_0)$  of the electric microfield the intensity maxima of the "combined Zeeman-Stark components" appears at wavelength distances  $\Delta \lambda > \Delta \lambda_z$ . A similar – but not so pronounced – feature was quantitatively obtained for  $H_\alpha$  [5]. The exact position of the intensity maximum as a function of  $B$  and  $N_e$  can theoretically only be obtained by solving completely the line broadening in the presence of a magnetic field as it was done for Ly  $\alpha$ , Ly  $\beta$  and  $H_\alpha$  [3–4]. For constant electric and magnetic fields the effect is theoretically demonstrated in Ref. [27].

#### 5. Conclusion

The line profiles of  $H_\beta$  emitted from an afterglow plasma imbedded in a strong magnetic field showed:

(i) electron density-dependent wavelength positions of the two lateral intensity maxima resulting from combined Stark-Zeeman components in the sense that the actual splitting increases with increasing electron density until the line profile is entirely dominated by Stark broadening. Only for very low electron densities the usual Zeeman splitting is found;

(ii) an irregular "satellite structure". Although the general form of this structure depends on magnetic induction and also slightly on electron density  $N_e$  we could not detect any characteristic change of the peak positions with  $N_e$ .

Measurements of  $H_\beta$  made without magnetic field but under otherwise unchanged experimental conditions also showed a "satellite structure" of pressure-dependent intensity.

In both cases we have interpreted the structure features as being due to  $H_2$  molecular lines. This interpretation has consequences with regard to the so-called dynamical Stark effect splitting.



Several authors (see Refs. [28–36]) have observed peak structures superposed on the line profiles of the Balmer lines  $H_\alpha$ ,  $H_\beta$  and  $H_\gamma$  which were in all cases interpreted as plasma satellites due to plasma turbulence. In the light of our new measurements it would be useful to repeat earlier published measurements with higher spectral resolution and to check the interpretation. We believe that in a number of cases the authors have seen  $H_2$  molecular transitions but under quite different excitation conditions. The strongest proof for this are the structures found in the profile of  $H_\gamma$  by Pease [36]. With a few exceptions, all peaks coincide with the wavelengths of  $H_2$  molecular lines listed in Ref. [19]. These few exceptions could represent  $He_2$  or  $HeH$  molecular lines, since the plasma was composed of a mixture of  $H_2$  and  $He$ . The strongest peaks just correspond to the wavelengths of the most intense  $H_2$  molecular lines.

In all other papers the spectral resolution of the published profiles is so low that a quantitative comparison with the  $H_2$  molecular spectrum is not possible, with the exception of Ref. [35]. The peak structure published in Ref. [35] could not be reproduced and has to be replaced by the present results of Figure 8.

\* *Note added in proof:* In the meantime appeared the english translation of a paper by A. I. Zhuzhunashvili and E. A. Oks [Zh. Eksp. Teor. Fiz. 73, 2142 (1977) — Sov. Phys. JETP 46, 1122 (1977)] who calculated broadening and satellite structure of several hydrogen Balmer lines due to combined action of quasistatic and turbulent fields. On the basis of their results they offered an “incontrovertible interpretation of the experimental data” obtained by Rutgers and Kalfsbeek [34] and Gallagher and Levine [31, 33]. In our opinion, the interpretation of the experimental data might be simpler. Unfortunately, the spectral resolution was not better than 0.5 Å. Despite this low resolving power surprising coincidences exist between measured peak positions and known  $H_2$  molecular wavelengths. It is not the place here to analyze the data in detail; only a few values shall be mentioned. In Ref. [31] the  $H_\delta$  profile shows a strong peak between  $\Delta\lambda \approx -28$  Å and  $\Delta\lambda \approx -33$  Å from the line center situated  $\lambda_0 = 4101.73$  Å. The most intense  $H_2$  molecular lines in that region are found between 4069.6 Å and 4074.1 Å, see [19]. The  $H_\gamma$  profile published in Ref. [34] has a peak structure asymmetric in intensity with respect to the line center situated at  $\lambda_0 = 4340.46$  Å. The strongest peak occurs at  $\Delta\lambda = -6.5 \pm 0.5$  Å. The strongest  $H_2$  molecular lines in that region have wavelengths  $\lambda = 4332.6$  Å; 4333.6 Å; 4334.7 Å; 4335.5 Å, in agreement with the measurement. The next intense  $H_2$  lines are situated at  $\lambda = 4336.3$  Å in agreement with a measured peak at  $\Delta\lambda = -4.5 \pm 0.5$  Å. The peak structure of  $H_\beta$  as measured by Rutgers and Kalfsbeek [34] shows strong similarity with our profile in Figure 12. The peak labeled 2 in Fig. 9 of Ref. [34] seems to correspond to our peaks  $\lambda = 4860.349 \dots 4860.791$  Å in Figure 12. Also the other peaks agree within the large experimental uncertainty with known  $H_2$  molecular wave-

lengths. — In our opinion, there are sufficient indications to doubt the interpretation offered by Zhuzhunashvili and Oks.

It might be possible that rotational lines associated with electronic transitions will be seen in the spectra of many other plasma sources provided observation is pushed sufficiently far into the line wings of corresponding atomic lines. The best candidates are compounds having high dissociation and/or ionisation energies such as CO,  $CO^+$ ,  $N_2$ ,  $N_2^+$ . Even at relatively high temperatures small admixtures of such gases may still lead to non-negligible perturbations of the profiles of atomic lines. But also molecular lines of impurities such as water and hydrocarbons may under appropriate thermodynamic conditions eventually lead to peak structures in the wing of atomic lines. A study of the dynamic Stark effect due to plasma turbulence should therefore be accompanied by a study of molecular lines which could mask the turbulence effect\*.

### Acknowledgement

The technical help of Mr. E. Sablon during the preparation of the experiment and the exploitation of the numerous oscillogrammes is gratefully acknowledged.

lengths. — In our opinion, there are sufficient indications to doubt the interpretation offered by Zhuzhunashvili and Oks.

In a short note Piel and Richter [Z. Naturforsch. 34a, 516 (1979)] claim to correct earlier measurements of Ramette and Drawin [35] and to explain the structure found in the  $H_\beta$  profile as being due to  $H_2$  molecular lines. We would like to point out that we already revised our earlier results in the sense that the structure originates from hydrogen molecule lines (see page 1291 of [14]). In the *note added in proof* to the same paper [14] we also proposed that the structure found by Burgess et al. in the  $H_\alpha$  profile — similarly as in our case for  $H_\beta$  — has probably its origin in  $H_2$  molecular transitions too. The present paper and especially the figure 12 contain the experimental details announced in [14].

- [1] E. K. Maschke and D. Voslamber, Proc. Intern. Conf. on Phenomena in Ionized Gases, Belgrad 1965: contributed paper, Vol. II, p. 568; also Report EUR-CEA-FC-354, Fontenay-Aux-Roses 1966: Stark Broadening of Hydrogen Lines in Strong Magnetic Fields.
- [2] Nguyen-Hoe, L. Herman, and H. W. Drawin, Z. Naturforsch. 21a, 1515 (1966).
- [3] Nguyen-Hoe, H. W. Drawin, and L. Herman, J. Quant. Spectr. Radiat. Transfer 7, 429 (1967).
- [4] Nguyen-Hoe, H. W. Drawin, and L. Herman, Report CEA-R-3161 Fontenay-Aux-Roses and Report EUR-3245f, EURATOM, Bruxelles: Profiles des Raies Spectrales Ly  $\alpha$ , Ly  $\beta$ , et  $H_\alpha$  de l'Atome H en Présence d'un Champ Magnétique dans un Plasma.
- [5] Nguyen-Hoe and H. W. Drawin, Z. Naturforsch. 28a, 789 (1973).

- [6] V. F. Aleksin and V. M. Fesenko, *Radio Engin. Electr. Physics* **12**, 1516 (1967).
- [7] H. W. Drawin, Report EUR-CEA-FC-481, Fontenay-Aux-Roses 1968: Stark-Broadening in the Presence of Magnetic Fields.
- [8] H. W. Drawin, H. Henning, L. Herman, and Nguyen-Hoe, *J. Quant. Spectr. Radiative Transfer* **9**, 317 (1969).
- [9] Yu. I. Galushkin, *Sov. Astronomy — A. J.* **14**, 301 (1970).
- [10] R. C. Isler, *Phys. Rev. A* **14**, 1015 (1976).
- [11] H. W. Drawin, L. Herman, and Nguyen-Hoe, Report EUR-CEA-FC-321, Fontenay-Aux-Roses 1965: Measurement of Broadened Lines from Plasma in the Presence of Strong Magnetic Fields.
- [12] P. Belland, H. W. Drawin, and H. O. Tittel, *Z. Physik* **222**, 372 (1969).
- [13] H. W. Drawin and J. Ramette, Report EUR-CEA-FC-963, Fontenay-Aux-Roses 1978: Investigation of the Structure of the HeI  $4^3D, ^3F-2^3P$  ( $\lambda = 447.15$  nm,  $\lambda = 447.0$  nm) Spectral Line Emitted from a Low Pressure Plasma.
- [14] H. W. Drawin and J. Ramette, *Z. Naturforsch.* **33a**, 1285 (1978).
- [15] D. D. Burgess and R. Mahon, *J. Phys. B* **5**, 1756 (1972).
- [16] P. Kepple and H. R. Griem, *Phys. Rev.* **173**, 317 (1968).
- [17] P. Kepple, Report N° 831, Center for Theoretical Physics, University of Maryland 1968; Improved Stark Profile Calculations for the First Four Members of the Hydrogen Lyman and Balmer Series.
- [18] H. W. Drawin and J. Ramette, *Z. Naturforsch.* **29a**, 838 (1974).
- [19] H. M. Crosswhite, *The Hydrogen Molecule Wavelength Tables of Gerhard Heinrich Dieke*, Wiley Intersc., New York 1972.
- [20] T. E. Sharp, *Atomic Data* **2**, 119 (1971).
- [21] F. H. Crawford, *Rev. Mod. Phys.* **6**, 90 (1934).
- [22] G. Herzberg, *Molecular Spectra and Molecular Structure*, Vol. I: Spectra of Diatomic Molecules, 2nd Ed., D. Van Nostrand Comp., New York 1950.
- [23] W. Jevons, *Band Spectra of Diatomic Molecules*, Physical Society, London 1932.
- [24] W. Weizel, *Bandenspektren*, Akademische Verlagsgesellschaft, Leipzig 1931.
- [25] A. Schadee, *J. Quant. Spectr. Radiat. Transfer* **19**, 517 (1978).
- [26] R. A. Hill, *J. Quant. Spectr. Radiat. Transfer* **7**, 401 (1967).
- [27] L. Herman, Nguyen-Hoe, H. W. Drawin, B. Petropoulos, and C. Deutsch, *Proc. 7th Intern. Conf. on Phenomena in Ionized Gases*, Vol. I, p. 562, Beograd 1966. C. Deutsch, H. W. Drawin, L. Herman, and Nguyen-Hoe, *J. Quant. Spectr. Radiat. Transfer* **8**, 1027 (1968).
- [28] C. C. Gallagher and M. A. Levine, *Phys. Rev. Letters* **27**, 1693 (1971).
- [29] A. B. Berezin, L. V. Dubovoi, B. V. Lyublin, and D. S. Yakovlev, *Soviet Phys. — Techn. Phys.* **17**, 750 (1972).
- [30] D. G. Yakovlev, *Soviet Phys. — Tech. Phys.* **17**, 1248 (1972/1973).
- [31] C. C. Gallagher and M. A. Levine, *Phys. Rev. Letters* **30**, 897 (1973).
- [32] W. R. Rutgers and H. de Kluiver, *Z. Naturforsch.* **29a**, 42 (1973).
- [33] C. C. Gallagher and M. A. Levine, *J. Quant. Spectr. Radiative Transfer* **15**, 275 (1975).
- [34] W. R. Rutgers and H. W. Kalfsbeek, *Z. Naturforsch.* **30a**, 739 (1975).
- [35] J. Ramette and H. W. Drawin, *Z. Naturforsch.* **31a**, 401 (1976).
- [36] D. C. Pease, Master Thesis, Plasma Physics Laboratory, The University of Texas at Austin: An Experimental Study of High Frequency Plasma Wave Effects in Hydrogen.